First-principles modeling of paramagnetic Si dangling-bond defects in amorphous SiO_2

András Stirling[1,*] and Alfredo Pasquarello[2,3]
[1]*Institute of Isotope and Surface Chemistry, Chemical Research Center, Hungarian Academy of Sciences, Budapest, P.O.B. 77, H-1525, Hungary*
[2]*Institut de Théorie des Phénomènes Physiques (ITP), Ecole Polytechnique Fédérale de Lausanne (EPFL), CH-1015 Lausanne, Switzerland*
[3]*Institut Romand de Recherche Numérique en Physique des Matériaux (IRRMA), CH-1015 Lausanne, Switzerland*
(Received 28 August 2002; published 4 December 2002)

We modeled paramagnetic Si dangling-bond defects in amorphous SiO_2 using a generalized-gradient density-functional approach. By creating single oxygen vacancies in a periodic model of amorphous SiO_2, we first generated several model structures in which the core of the defect consists of a threefold coordinated Si atom carrying a dangling bond. These model structures were then fully relaxed and the hyperfine parameters calculated. We found that the hyperfine parameters of such model defects, in both the neutral and positive charge states, reproduced those characteristic of the E', in accord with experimental observations for amorphous SiO_2. By eliminating a second O atom in the nearest-neighbor shell of these defect centers, we then generated model defects in which the Si atom carrying the dangling bond forms bonds with two O atoms and one Si atom. In this defect, the spin density is found to delocalize over the Si-Si dimer bond, giving rise to two important hyperfine interactions. These properties match the characteristics of the hyperfine spectrum measured for the *S* center. Our results are complemented by the calculation of hyperfine interactions for small cluster models which serve the threefold purpose of comparing different electronic-structure schemes for the calculation of hyperfine interactions, estimating the size of core-polarization effects, and determining the reliability of cluster approximations used in the literature.

DOI: 10.1103/PhysRevB.66.245201 PACS number(s): 61.72.Bb, 61.43.Fs, 76.30.−v, 71.15.−m

I. INTRODUCTION

E'-type paramagnetic defects have attracted a great deal of attention because of their responsibility in affecting the quality of Si-based electronic devices with SiO_2 as gate material.[1,2] The basic kernel of E'-type centers consists of a $\cdot Si{\equiv}O_3$ unit, in which the $\cdot$ symbol represents an unpaired electron. Among these defects, the variant occurring in amorphous SiO_2 is most commonly referred to as E'_γ and is generally associated to a deep hole trap.[1,3]

For the E'_1 center, the analog of this center in α quartz, Feigl, Fowler, and Yip[4] proposed a successful model which is nowadays generally accepted. This model consists of a positively charged and asymmetrically relaxed oxygen vacancy. The unpaired electron is localized on one of the Si atoms facing the vacancy ($\cdot Si{\equiv}O_3$), while the other Si atom undergoes a significant relaxation and binds to a distant O atom, giving rise to a puckered structure with a positively charged threefold coordinated O center ($O^+{\equiv}Si_3$).[5]

On the basis of the similar electron-spin-resonance (ESR) properties, an analogous defect structure was proposed for the E' centers in the amorphous state.[6,7] However, several experimental measurements indicate that there is no direct correlation between positive charge and E'-type paramagnetic defects in amorphous SiO_2.[3,8–14] In particular, neutral E'_γ-like defect sites have been found in SiO_2 films prepared by plasma-enhanced chemical vapor deposition followed by electron transport across the deposited film,[9] and in thermal SiO_2 thin films exposed to vacuum-ultraviolet and/or ultraviolet light.[3,10] In other cases, the neutral E'-type defects have been linked to an analog of the E'_β center,[8,11] identified by Griscom in bulk fused silica.[15,16] More recently, other models for the E'_γ center have been explored,[17,18] but have not yet found additional confirmation.

In oxygen-deficient vitreous SiO_x ($0<x<2$) a series of E'-type variants have been postulated,[2,19,20] which consist of Si dangling-bond centers with core fragments defined by $\cdot Si{\equiv}SiO_2$, $\cdot Si{\equiv}Si_2O$, and $\cdot Si{\equiv}Si_3$. Among these units, the $\cdot Si{\equiv}Si_3$ structure corresponds to the composition of the P_b-type defects at Si-SiO_2 interfaces (see Ref. 21, and references cited therein). The intermediate constitutions, $\cdot Si{\equiv}SiO_2$ and $\cdot Si{\equiv}Si_2O$, were first assumed in SiO_x with oxygen substoichiometry by Holzenkämpfer *et al.*, who observed a characteristic dependence of the effective *g* value on the oxygen content.[19] Griscom found a paramagnetic defect, which he called the *S* center, in phosporus-doped silica glass,[20] and assigned this center to the two E'-type variants of intermediate composition on the basis of similar Zeeman lines. Unfortunately neither of these assignments could be considered conclusive since no hyperfine or *g* anisotropy measurements were performed on this defect. The *S* center was later also investigated by Stesmans *et al.* both in thermal SiO_2 after postoxidation vacuum annealing and in fused silica exposed to gaseous SiO molecules.[22–24] The defect is characterized by an isotropic ESR signal and a blurred hyperfine doublet with a splitting of 279 ± 12 G.[24] Moreover, at the borderline of experimental accuracy, another much weaker hyperfine doublet could be detected with a splitting of 162 ± 5 G.[24] Hosono and Weeks also identified an oxygen-deficient paramagnetic center in Cr-doped vitreous silica,[25] which they called the *X* center. They assigned this defect to an E'-type structure of $\cdot Si{\equiv}SiO_2$ composition,

and suggested that *X* and *S* centers were identical. Recently, the hyperfine interaction of the *X* center was measured in Si implanted amorphous SiO_2.[26] A hyperfine doublet with a splitting of 230 G was assigned to $\cdot Si{\equiv}Si_nO_{3-n}$ units with *n* equal to 1 or 2. This observation provides additional support for the assignment of the *X* center to an intermediate E'-type variant, since the measured hyperfine interaction falls between those of the E'_γ (419 G) (Ref. 6 and 27) and of the P_b-type centers (100–127 G).[21] On the other hand the discrepancy between the hyperfine splittings of the *S* and *X* centers questions the hypothesis of their structural identity.[24] Note that the $\cdot Si{\equiv}Si_2O$ structure was also proposed as a possible kernel for the P_{b1} defect at the $Si(100)$-SiO_2 interface.[21,28,29] Very recently, however, the atomic structure of the P_{b1} center has been convincingly interpreted in terms of a $\cdot Si{\equiv}Si_3$ central core, similarly to the other P_b-type centers.[30]

From the theoretical side, the *S* and *X* centers have been given only modest attention, wheareas the E' center both in α quartz and in amorphous SiO_2 has been the subject of numerous semiempirical[5,31–33] and *ab initio* calculations.[17,18,34–47] Among the *ab initio* studies, only a few addressed ESR parameters[17,18,35,39,40,45,46] and even less aimed at modeling the amorphous environment.[17,18,35,39–41] Karna and Kurtz[40,42] performed Hartree-Fock calculations on very small model clusters to predict hyperfine data for the E' center and its oxygen-deficient variants. Pacchioni and Vitiello addressed the E' center using similar clusters and a hybrid gradient-corrected density-functional methodology.[39] Using cluster calculations, Uchino *et al.* showed that their alternative model for the E' center also reproduced the experimental hyperfine splittings.[17,18] Boero *et al.* studied a model for the E'_γ center within a density-functional approach starting from a periodically repeated model structure of vitreous SiO_2 generated by first-principles molecular dynamics.[35]

The theoretical treatment of defects in disordered systems is not only hindered by the inherent statistical nature of the problem, but is also limited, more practically, by the neccessity of using a large number of atoms to account for structural relaxations. In *ab initio* investigations, two approaches are generally in use for investigating defect centers in amorphous environments. The first approach makes use of large cluster models,[17,18,36–42] while the second one relies on defective crystalline models.[34,45,46] However, neither of these approaches appropriately reproduces the amorphous environment. Only recently has it become possible to model defects in a realistic amorphous environment through the use of large periodically repeated supercells in which the disorder is reproduced within the unit cell.[35,44]

A major obstacle in the interpretation of experimental ESR lines is associated with the use of different electronic-structure methods in the literature. While density-functional theory (DFT) is becoming the preferred framework for studying systems with a large number of atoms, a variety of different implementations are currently in use. Cluster models are generally dealt with by quantum chemical methods based on localized basis sets, while basis sets of plane waves are usually preferred in periodic calculations. While these methods yield in most cases essentially equivalent results for energies and structural parameters, their capability in providing reliable hyperfine parameters is less well established.

In the present study, we address paramagnetic Si dangling-bond defects in amorphous SiO_2, using a density-functional approach. Our aim is to calculate hyperfine parameters on realistic model structures of oxygen mono- and divacancy centers, in order to assign experimentally observed ESR lines. We adopt as a starting point the same periodically repeated model structure of vitreous SiO_2 (Ref. 48), as used by Boero *et al.*[35] We first model E'_γ defect centers by defects with $\cdot Si{\equiv}O_3$ core units to assess the accuracy of our approach. In particular, we focus on the charge state of the E'_γ center in amorphous SiO_2. We find that, insofar as the structural unit $\cdot Si{\equiv}O_3$ is preserved as the core of the defect center, the hyperfine parameters are practically unaffected by the charge state of the center, in accord with experimental observations.[15] Our calculated hyperfine interactions for defect centers containing the $\cdot Si{\equiv}SiO_2$ core unit are in good agreement with those measured for the *S* center. In particular, our calculations reveal an interesting spin-delocalization effect across the Si-Si bond. This spin redistribution yields two different and well-separated hyperfine signals, which may constitute a distinctive feature for the experimental characterization of this defect. Indeed, very recent measurements show some evidence in favor of two hyperfine signals associated to the *S* center.[24] Finally, we complement our study by calculating hyperfine interactions for small cluster models using various electronic-structure methods. The purpose of these model calculations is threefold. First, we compare hyperfine interactions calculated within the Hartree-Fock approximation and a density-functional generalized-gradient approximation. Second, using all-electron methods and comparing with pseudopotential methods, we could estimate the contribution to the hyperfine interaction resulting from core polarization. Third, we identified a series of issues which should be carefully considered when adopting small cluster approximations.

This paper is organized as follows. Section II gives computational details of the methods used in this work. Sections III and IV are devoted to the study of Si dangling-bond defects with $\cdot Si{\equiv}O_3$ and $\cdot Si{\equiv}SiO_2$ core units, respectively. In Sec. V, the results for small cluster models are discussed. The conclusions are given in Sec. VI.

II. COMPUTATIONAL DETAILS

The electronic structure in our work was treated within a density-functional approach,[49] in which the Perdew-Wang 1991 (PW91) generalized-gradient approximation (GGA) was used for the exchange-correlation energy.[50] Electronic and structural relaxations were achieved by performing damped Car-Parrinello molecular dynamics.[51] The electronic wave functions were expanded on a basis of plane waves. The interaction between the valence electrons and the ionic cores was described with ultrasoft pseudopotentials[52] (PPs) for both Si and O atoms. The use of an ultrasoft PP for Si is motivated by the necessity of calculating accurate ESR parameters. We found that the reconstruction of the all-electron

density at the nucleus site was more accurate with an ultrasoft than with a norm-conserving PP for Si.[30] We used energy cutoffs of 25 and 150 Ry for the valence wave functions and the augmented charge density, respectively. Test calculations showed that these energy cutoffs yield good convergence in the calculated properties. The Γ point was used for sampling the Brillouin zone. An extensive description of the applied methodology is given in Ref. 53.

In this work, we used as a starting point a model structure previously obtained by first-principles molecular dynamics.[48] This model contains 24 SiO_2 units at the experimental density in a periodically repeated cubic cell, and consists of a chemically ordered network of corner-sharing tetrahedra. For a more detailed analysis of the structural properties of this model, we refer to Ref. 48 for parameters such as bond lengths and angles, and to Ref. 54 for a description in terms of ring statistics. This model has also successfully been used for a series of studies involving the vibrational properties of vitreous silica.[54,55]

The model structure was originally obtained in the local-density approximation (LDA) for the exchange-correlation energy.[48] The use of a GGA functional led to a slight increase in the Si-O bond length which was accommodated by small rotations of the SiO_4 tetrahedra. To preserve the original bond angles, we therefore scaled the volume of the supercell consistently with the Si-O bond length. This yielded a model structure with a density of 2.14 g/cm^3, still very close to the experimental density of amorphous SiO_2 (2.20 g/cm^3).

The defect models were obtained by creating oxygen vacancies in this undefected structure and by allowing for full relaxation of the atomic structure. When a vacancy model was positively charged, a uniform negative background restored the charge neutrality in the supercell. The cluster calculations, which were performed with the same PP method, made use of a cubic simulation cell of side $L=11$ Å, sufficiently large to neglect interactions between periodic images. The structure of the clusters was always fully relaxed.

The ^{29}Si hyperfine splitting in the ESR spectrum is described by the hyperfine Hamiltonian, $H=\mathbf{S}\cdot\mathbf{A}\cdot\mathbf{I}$, where the hyperfine tensor $\mathbf{A}$ accounts for the coupling between the electronic ($S=1/2$) and nuclear ($I=1/2$) spins. The components of $\mathbf{A}$ can be written as $A_{ij}=a\,\delta_{ij}+b_{ij}$, where the dominant term, the contact interaction, is expressed as

$$a=\frac{8\pi}{3}g_e\mu_e g_{\mathrm{Si}}\mu_{\mathrm{Si}}\rho_s(\mathbf{R}). \tag{1}$$

Here $\rho_s(\mathbf{R})=\rho_\uparrow(\mathbf{R})-\rho_\downarrow(\mathbf{R})$ is the electron-spin density at the nucleus site $\mathbf{R}$, g_e is the free-electron g factor, μ_e is the Bohr magneton, g_{Si} is the nuclear gyromagnetic ratio for Si, and μ_{Si} is the corresponding nuclear magneton. Note that, although μ_{Si} assumes negative values, we here give the hyperfine interactions as positive values, since only the absolute values are experimentally accessible. Negative theoretical values indicate excess minority-spin density. The parameters b_{ij} result from the dipolar-dipolar interaction term. Due to the isotropic nature of the amorphous system under consideration, the contribution of the direction-dependent b_{ij} terms vanishes. Therefore, we here only focused on the isotropic contact term a.

The calculation of a requires the accurate value of the spin density at the nucleus site, which is, however, not directly provided in our PP calculations. Several procedures have been proposed and successfully applied for recovering all-electron wave functions and densities from their PP counterparts.[30,35,45,56,57] Here we apply a scheme which we previously derived for the ultrasoft PP method and which has successfully been used in the context of P_b-type centers at Si-SiO_2 interfaces.[30] Within the ultrasoft PP method,[52] the spin-up and spin-down densities can be written as

$$\rho^s(\mathbf{r})=\sum_i\left[|\phi_i^s(\mathbf{r})|^2+\sum_{nm,I}Q_{nm}^I(\mathbf{r})\langle\phi_i^s|\beta_n^I\rangle\langle\beta_m^I|\phi_i^s\rangle\right], \tag{2}$$

where s labels the spin state, the ϕ_i^s are the one-electron spin-dependent pseudowave functions, and the β_n^I and $Q_{nm}^I(\mathbf{r})$ are projector and augmentation functions, respectively. In Eq. (2), the first term in the brackets describes the *soft* part of the electron density while the second term corresponds to the *hard* contribution which is strictly localized in the core region.[53] In the actual PP calculations, pseudized $Q_{nm}^I(\mathbf{r})$ augmentation functions are used.[53] When the electron density around a given nucleus is reconstructed, the pseudized $Q_{nm}^I(\mathbf{r})$ are replaced with their original counterparts. In this way, we recover the detailed *valence* electron density in the core region, and, in particular, at the site of the nucleus. We note that, since core states are only treated implicitly, core-polarization effects cannot be accounted for in our formulation. An estimate for this neglected effect is found in Sec. V. Furthermore, our formulation also neglects relativistic effects, which are, however, expected to be small for silicon.[58]

In our study of small cluster models, we also used two *all-electron* electronic-structure methods, DMOL (Ref. 59) and GAUSSIAN 98 (G98),[60] available as commercial software packages. In the G98 calculations, we used the same PW91 exchange-correlation functional as in the PP calculations.[50] The DMOL code is not provided with the PW91 exchange-correlation functional. We therefore used another exchange-correlation functional which differs from the PW91 functional by the use of an exchange functional due to Becke.[61] Test calculations with the G98 code showed that these two functionals yield negligible differences as far as the hyperfine parameters are concerned. In the following, we therefore consider that the hyperfine results obtained with our PP method and the two all-electron methods all result from the *same* density-functional scheme. Differences between the results should be attributed to the implicit treatment of core states in the PP method or to the incompleteness of the basis sets in the all-electron methods. To minimize the latter effect, we chose relatively large basis sets in the all-electron calculations: 6–311+G* in G98 and double numerical plus polarization functions in DMOL.[62]

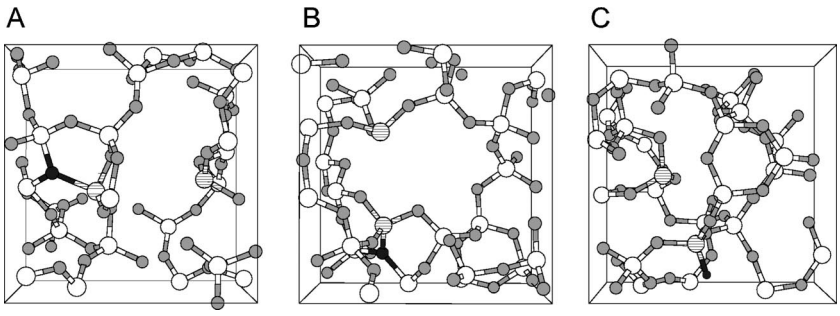

FIG. 1. Relaxed structures of the three model defects featuring a $\cdot Si{\equiv}O_3$ core unit. Si atoms are in white, O atoms in gray, and threefold coordinated oxygen atoms (A and B) and the extra H atom (C) in black. The Si atoms facing the vacancy are dashed.

III. THE $\cdot Si{\equiv}O_3$ DEFECT CENTER

First, we addressed the E'_γ defect, of which the assignment to a Si dangling bond is generally accepted, in order to assess the accuracy of our methodology. We modeled the E'_γ defect by creating charged oxygen vacancies in our model structure of vitreous silica. We considered two possible locations for the defect, which gave rise to model A and B upon structural relaxation (Fig. 1). In particular, model B corresponds to the defect structure studied in Ref. 35, which we reconsidered because of the different technical ingredients in the present work. The location of this defect was selected according to the criterion that a suitably located oxygen atom be present for the stabilization of the puckered configuration through the formation of a dative bond.[35] The location of the defect in model A was identified according to the same criterion. Complete structural relaxations yielded approximately tetrahedral configurations around the paramagnetic Si atom in both cases, the O-Si-O bond angles showing small variations around the average value of 108.1° for model A and of 109.1° for model B. The distances between the puckered Si atom and the threefold coordinated oxygen atom are 1.99 and 1.89 Å, respectively, indicating weak covalent bond formation in both cases.

For the relaxed model structures, we obtained isotropic hyperfine interactions of 517 and 485 G (Table I). The Si atoms which underwent the puckering distortion were found to carry no spin density, as expected for atoms with saturated valence shells. The calculated hyperfine interactions overestimate the measured value (419 G) (Ref. 6) by 23% (A) and 16% (B). The use of the PW91 functional only slightly improves the agreement (22%) obtained previously for model B within the LDA and with a different reconstruction procedure for the electron density.[35] In view of the results in Sec. V, core-polarization effects are negligible (about 1%) for a defect with a $\cdot Si{\equiv}O_3$ core unit. The residual error should be attributed to a deficiency of our theoretical scheme for the description of the electronic structure, which could result from an improper description of the exchange and correlation energy or from the neglect of relativistic effects.[45,58]

TABLE I. Hyperfine interaction a_{HF} for model structures with a $\cdot Si{\equiv}O_3$ core unit (Fig. 1).The charge state is given in parentheses. The SHF contact values averaged over the first-neighbor Si atoms ($\bar{a}_{\mathrm{SHF}}$) and the distance $d_{\mathrm{Si\text{-}Si}}$ between the Si atoms adjacent to the vacancy are also given (in Å). The calculated hyperfine values are compared with experimental data for the E'_γ defect (Refs. 6 and 63). Hyperfine parameters are in Gauss.

	Model A(+)	Model B(+)	Model C(0)	Experiment
a_{HF}	517	485	495	419[a]
$\bar{a}_{\mathrm{SHF}}$	9	14	11	13[a,b]
$d_{\mathrm{Si\text{-}Si}}$	4.62	4.35	3.74	

[a]Reference 6.
[b]Reference 63.

We also calculated superhyperfine (SHF) interactions associated to first-neighbor Si atoms. The averages of these SHF interactions in model A (9 G) and B (14 G) are in good quantitative agreement with the experimental feature at 13 G (see Table I).[6] This lends strong support to the interpretation of this feature in terms of a ^{29}Si SHF interaction[63] rather than in terms of an effect due to protons.[6] This assignment is further supported by analogy with the E'_1 center where features at about 8 G (Ref. 64) have been convincingly assigned to SHF interactions.[35] We note that the agreement between theoretical and experimental SHF interactions appears noticeably improved by the use of a PW91 functional with respect to the LDA one.[35] A similar improved GGA description of SHF interactions was also achieved for the E'_1 center.[45] Overall, the present results indicate that our methodology properly gives the electron-spin density of Si dangling-bond defects, not only at the site of the miscoordinated Si atom but also at further distances, corresponding to first Si neighbors.

We then investigated whether the E'_γ line could also result from an oxygen vacancy in the *neutral* charge state. We created a neutral oxygen vacancy by coordinating the puckered silicon atom with an extra hydrogen atom instead of with a network oxygen atom (model C, Fig. 1). In this case, a saturated bonding configuration of the puckered Si atom is obtained, while the dangling bond on the defect Si atom remains singly occupied and in a paramagnetic state. Upon relaxation, we again obtained a tetrahedral configuration for the defect Si atom with an average O-Si-O bond angle of 107.0°. The other Si atom which faced the vacancy forms a normal covalent bond of 1.49 Å with the extra hydrogen atom. The distance between the two Si atoms facing the vacancy is in this case somewhat shorter than for the charged model structures, because the Si atom undergoing the distortion is already saturated by the hydrogen atom and does not need to form a bond with a network oxygen atom. For this configuration, we calculated a hyperfine splitting of 495 G, which falls in between the values for models A and B and compares well with experiment (Table I). The average of the

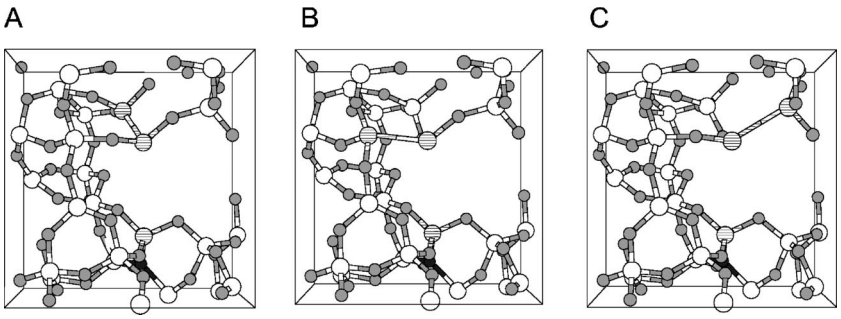

FIG. 2. Relaxed structures of the three model defects featuring a $\cdot Si{\equiv}SiO_2$ core unit. Si atoms are in white, O atoms in gray, and threefold coordinated oxygen atoms in black. The Si atoms facing the vacancy are dashed.

SHF interactions shows a similar good agreement with the other models and with experiment.

The agreement between the hyperfine interactions of the charged and neutral models can be understood by considering the significant distance between the Si atoms facing the vacancy. In the positively charged models, the Si atom which carries the dangling bond and gives the paramagnetic response is located at distances of about 6 Å from the threefold coordinated oxygen atom, where the charge is localized. At these distances, the spin density on the defect Si atom is evidently only marginally affected by the nearby presence of positive charge, yielding hyperfine parameters close to those of the neutral model.

The hyperfine interactions in our models are consistent with experimental observations on bulk silica and thin oxide films on silicon. For bulk a-SiO_2, Griscom showed that the E'_β and E'_γ defects, which differ by their g matrices, exhibit identical hyperfine spectra.[15,16] The E'_β is supposed to be a neutral E' variant featuring an isolated $\cdot Si{\equiv}O_3$ unit facing a small void in the amorphous SiO_2 structure.[1,15,16,65] ESR measurements on thin SiO_2 films also indicate that the basic $\cdot Si{\equiv}O_3$ kernel gives the same hyperfine signal irrespective of its charge state.[3,9,10] It follows that the paramagnetic characteristics of the E'_γ defect are not necessarily associated with the prior trapping of a hole.

IV. THE $\cdot$Si≡SiO$_2$ DEFECT CENTER

We could model E'-like oxygen divacancies by removing an additional oxygen atom from the first-neighbor shell of the defect Si atom in the models for E'_γ. In order to avoid undesirable rigidity around the defect site upon the formation of a covalent Si-Si backbond, we considered that the defect Si atom should not belong to five-membered rings or smaller.

TABLE II. Hyperfine interaction of the Si atom carrying the dangling bond (a_{HF}), and of its nearest-neighbor Si atom, (a^N_{HF}), for the model structures with a $\cdot Si{\equiv}SiO_2$ core unit (Fig. 2). Average values are compared with experimental values for the S (Ref. 24) and the X (Ref. 26) centers. The Si-Si^N distances are also given. Hyperfine parameters are given in Gauss and distances in Å.

	Model A	Model B	Model C	Average	S	X
a_{HF}	344	303	298	315	279	230
a^N_{HF}	158	206	241	202	162	
$d_{Si\text{-}Si^N}$	2.46	2.67	2.79			

With this criterion in view, we selected model B in Fig. 1 as the starting structure. By removing each of the three neighbor oxygen atoms separately, we created three different oxygen divacancy models. Figure 2 shows the configurations obtained upon full structural relaxation.

For the three model structures obtained in this way, the Si-Si distance between the defect Si atom and the Si atom in its first-neighbor shell, denoted Si^N, ranges between 2.4 and 2.8 Å (Table II). These values compare well with the Si-Si distance of about 2.5 Å calculated for a neutral dimer bond embedded in a SiO_2 network.[66] The large variation (around 0.3 Å) in the Si-Si^N bond lengths reflects the amorphous nature of the system. For each of the three models, the average bond angle around the Si^N atom lies within less than 1° from the tetrahedral angle of 109.5°. However, the average deviations (6.5°–12.8°) show that the bonding configurations around the Si^N atoms are considerably distorted by the Si-Si bond formation.

The second vacancy only has a slight effect on the structural parameters at the puckered side, as expected from the large distance (>4 Å) between the two silicon atoms facing the first oxygen vacancy. For instance, the distance between the threefold coordinated oxygen atom and the relaxed Si atom ranges between 1.84 and 1.86 Å for the three model structures, not distant from the original 1.89 Å. The structural models are all positively charged because of the presence of the threefold coordinated oxygen atom. However, in view of the results in the previous section, we consider that the influence of the charge state on the hyperfine parameters is negligible.

For each of the model structures, we calculated isotropic hyperfine interactions both for the defect Si atom and for its first-neighbor Si^N (Table II). The hyperfine interactions for the defect Si atoms are now lower than in the E'_γ models, ranging between 298 and 344 G. The decrease of the hyperfine interaction could be anticipated, since oxygen nearest neighbors are known to enhance the hyperfine splitting.[30] More unexpectedly, the spin density carried by the Si^N atoms is very significant, yielding hyperfine interactions (a^N_{HF}) between 158 and 241 G. The hyperfine interactions a_{HF} and a^N_{HF} correlate with the Si-Si^N distance: while a_{HF} decreases with the Si-Si^N distance, a^N_{HF} increases (Table II). These correlations are confirmed by the study of small model clusters (see below). We note that the absolute variation of a^N_{HF} with Si-Si^N distance is almost twice as large as for a_{HF}. These results therefore predict that the Si dangling-bond defect associated to a $\cdot Si{\equiv}SiO_2$ unit should present a hyperfine spec-

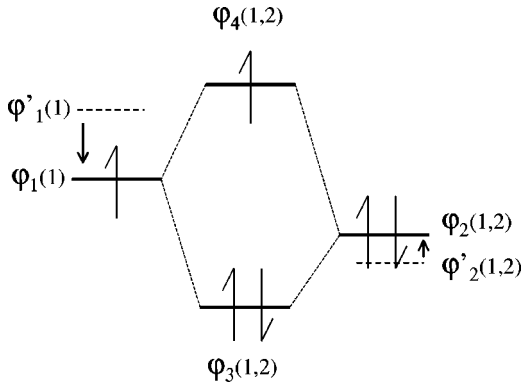

FIG. 3. Schematic orbital diagram representing the effect of the oxygen atoms on the energy levels associated to a $\cdot\mathrm{Si}\equiv\mathrm{SiO_2}$ core unit. $\varphi_1(1)$: initial dangling orbital; $\varphi_2(1,2)$: $\mathrm{Si_1}$-$\mathrm{Si_2}$ initial bonding orbital. Their overlap results in two new orbitals, φ_3 (basically the Si-Si bonding orbital) and φ_4 (the delocalized unpaired orbital). The numbers in subscripts indicate the origin of the atomic orbitals composing a φ_i molecular orbital: 1 for the defect Si atom and 2 for its Si first neighbor. φ_1' and φ_2' levels indicate the energy position of the corresponding orbitals in absence of oxygen atoms in the first-neighbor shell of the Si defect atom.

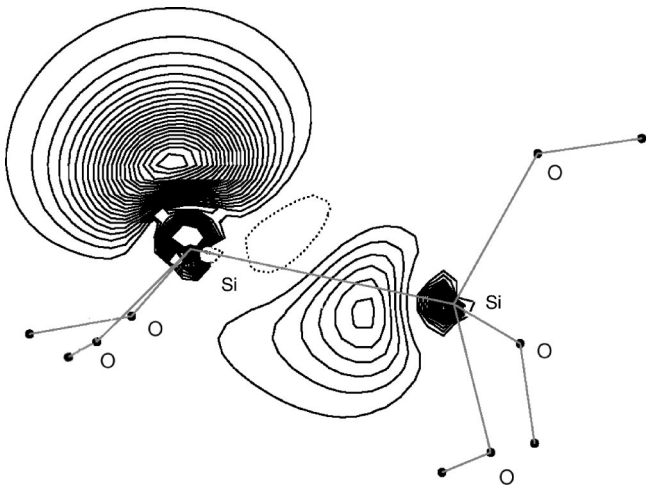

FIG. 4. Spin-density distribution for the Si dangling-bond defect containing a $\cdot\mathrm{Si}\equiv\mathrm{SiO_2}$ core unit as obtained from model cluster calculation.

trum consisting of *two doublets*, the doublet with the smaller splitting being broader because of its higher sensitivity to the distribution of Si-$\mathrm{Si^N}$ distances in amorphous $\mathrm{SiO_2}$.

To compare with available experimental data, we averaged the calculated hyperfine interactions for the three model structures, in order to reduce the statistical indetermination. We obtained average a_{HF} and $a_{\mathrm{HF}}^{\mathrm{N}}$ of 315 and 202 G, respectively (Table II). Given the observed dependencies on the Si-$\mathrm{Si^N}$ distance, our sampling appears quite insufficient for an accurate statistical estimate, particularly for $a_{\mathrm{HF}}^{\mathrm{N}}$. Nevertheless, useful indications can be obtained when these values are compared to experimental data. The present data appear consistent with the experimental characterization of the *S* center by Stesmans *et al.*[24] In particular, even some evidence for a hyperfine spectrum consisting of two doublets could recently be detected.[24] The dominant hyperfine interaction in our models (315 G) overestimates by 13% the experimental value (279 G),[24] consistent with the systematic tendency observed for our methodology.[30] The average of the $a_{\mathrm{HF}}^{\mathrm{N}}$ values overestimates the experimental value by 26%. This overestimation is somewhat larger than expected, but could result from nonrepresentative Si-$\mathrm{Si^N}$ distances in our model structures. In fact, the limited size of our model structures and the use of periodic boundary conditions might lead to strained Si-$\mathrm{Si^N}$ distances, which would enhance the $a_{\mathrm{HF}}^{\mathrm{N}}$ interactions. The apparent smaller intensity of the inner doublet[24] also appears consistent with the stronger sensitivity of this line to variations in the Si-$\mathrm{Si^N}$ distances. In the case of the *X* center, only a single hyperfine doublet has been reported.[26] The average a_{HF} of our models overestimates the observed splitting by as much as 37%. The absence of a second hyperfine doublet and the excessive overestimation of the hyperfine interaction suggest that the latter center results from a different atomic structure (cf. discussion in Ref. 24).

It is of interest to investigate the origin of the spin delocalization in the $\cdot\mathrm{Si}\equiv\mathrm{SiO_2}$ unit. The spin delocalization also occurs in small cluster models (Sec. V) and could therefore be studied with electronic-structure methods based on localized basis sets. Inspecting the electronic orbitals reveals that this effect results from the presence of two first-neighbor oxygen atoms, which strongly affect the Si-$\mathrm{Si^N}$ interaction. Due to their large electronegativity, the *p* character in the Si-O bonds is enhanced, leaving more *s* character on the defective Si atom, as compared to a normal sp^3 hybridization state.[67] Consequently, a slight increase of the *p* character in the Si-$\mathrm{Si^N}$ bond is observed because the defect Si atom has now an enhanced electronegativity. The enhanced *s* character in the dangling-bond orbital lowers its energy level, while the extra *p* contribution to the Si-$\mathrm{Si^N}$ bond lifts the bonding energy level associated to this bond. This effect gives rise to a significant interaction between the dangling-bond and the bonding Si-$\mathrm{Si^N}$ orbitals, as displayed in Fig. 3. This interaction is responsible for the formation of two molecular orbitals encompassing both Si atoms, the unsaturated defect atom and its saturated nearest neighbor. The observed spin delocalization can also be explained in terms of hyperconjugation.[68] In organic chemistry, hyperconjugation is a stabilizing interaction associated to charge transfer from a saturated bond, usually of type σ, to a *p*-type orbital.[68] In the present case, the stabilization results from an electron-density flow of minority spin from the Si-$\mathrm{Si^N}$ σ-type bonding orbital towards a hybrid dangling-bond orbital, yielding excess spin density on the saturated $\mathrm{Si^N}$ atom. Figure 4 displays the spin density in the plane defined by the Si-$\mathrm{Si^N}$ bond and the dangling-bond axis. The figure clearly shows the considerable spin density residing on the $\mathrm{Si^N}$ atom. The dominant part of the spin density is found on the defective Si atom, in a hybrid *s*-*p* orbital of enhanced *s* character. Some spin density is also found in the bonding region of the two silicon atoms.

The rationale given above also explains the trends of the hyperfine interactions with the Si-$\mathrm{Si^N}$ distance. In fact, the larger the Si-$\mathrm{Si^N}$ distance, the higher the energy level of the

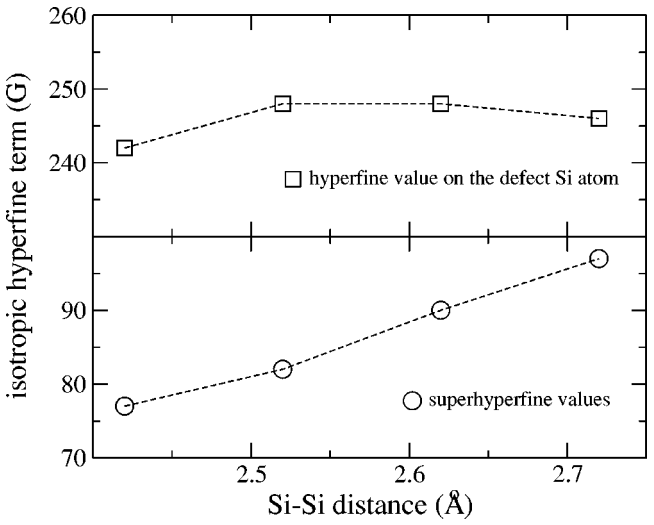

FIG. 5. Dependence of the isotropic hyperfine interactions on the Si-Si^N bond length for the $\cdot Si{\equiv}SiO_2$ defect center. The dashed lines are guides to the eyes.

bonding Si-Si^N orbital, and the higher the delocalization of the spin density. We studied this effect more systematically by taking as a model the $\cdot Si(OSiH_3)_2(SiH_3)$ cluster, which well reproduces the nearest-neighbor environment of the Si dangling bond. Using the same PP method as for the periodic models, we first optimized the geometry. Then, we considered structural configurations obtained by elongating the Si-Si^N bond while keeping all the other internal coordinates fixed. The calculated hyperfine interactions for the defect Si atom and for its Si neighbor Si^N are given as a function of the Si-Si^N distance in Fig. 5. It is seen that the hyperfine interaction a_{HF}^N associated to the Si^N atom increases drastically with the bond length, whereas the main hyperfine interaction a_{HF} of the defect is only marginally affected.

V. CLUSTER CALCULATIONS

So far, the modeling of the *S* and *X* centers has exclusively relied on Hartree-Fock calculations for small clusters.[40,42] In particular, an isotropic hyperfine interaction of 247 G was found for the $\cdot Si{\equiv}SiO_2$ unit, an estimate falling in between the experimental values of 230 and 279 G for the *X* (Ref. 26) and *S* (Ref. 24) defect centers, respectively. For comparison, the present density-functional calculations, which focused on the same defect unit but within periodic model structures, gave 315 G (Table II), favoring the assignment to the *S* center. Since the two theoretical estimates (247 and 315 G) are significantly different, we decided to perform additional cluster calculations.

In addition to our PP method, we used in the cluster investigation two different all-electron electronic-structure methods: DMOL (Ref. 59) and G98 (Ref. 60). This gave us the opportunity to address three issues. First, we compared hyperfine parameters calculated for the same model structures using different theoretical schemes, namely, the Hartree-Fock approximation and a GGA to DFT. Second, we could estimate the effect of neglecting core-polarization effects in our PP scheme by comparing with all-electron (AE) methods. In particular, such a study allowed us to compare hyperfine parameters calculated with different electronic-structure methods for the same structural models. Third, by comparing the hyperfine parameters of the cluster models with those obtained for periodic models, we could identify some aspects which could easily be overseen in modeling based on cluster calculations. Besides the usual finite-size effects, these also include strain and cage-polarization effects.

TABLE III. Hyperfine interactions (in Gauss) for model clusters as calculated within the Hartree-Fock and GGA-DFT schemes. In the case of the $\cdot Si{\equiv}Si_3$ cluster, the negative sign found for the SHF interaction indicates excess minority-spin density: for a discussion, see Ref. 72.

		Hartree-Fock	GGA-DFT
$\cdot Si{\equiv}Si_3$	a_{HF}	127	78
	a_{HF}^N	−13	−4
$\cdot Si{\equiv}Si_2O$	a_{HF}	174	129
	a_{HF}^N	10	14
$\cdot Si{\equiv}SiO_2$	a_{HF}	246	207
	a_{HF}^N	64	65
$\cdot Si{\equiv}O_3$	a_{HF}	411	389

A. Hartree-Fock vs density functional

To highlight the effect of the exchange and correlation interaction on the hyperfine parameters, we compared our density-functional scheme based on a GGA functional[50] with the Hartree-Fock scheme. For the calculations within both schemes, we adopted the G98 method, so that all differences could be attributed to the treatment of the exchange and correlation energy. We constructed a series of clusters $\cdot Si(SiH_3)_{3-x}(OSiH_3)_x$ (with $0 \leqslant x \leqslant 3$), in which the central silicon atom carries a dangling bond and the terminations model a varying number of oxygen atoms in its first-neighbor shell. The structures of all clusters were fully relaxed according to the adopted theoretical scheme.[69]

Table III gives the hyperfine parameters for these clusters as calculated with the Hartree-Fock and GGA-DFT schemes. The Hartree-Fock scheme clearly yields much larger hyperfine values than the GGA-DFT scheme. The difference between the two schemes decreases from 63% to 6% as the numbers of the surrounding oxygen atoms increase from 0 to 3. For the SHF interactions, the deviations are not as systematic but also show a decreasing trend.

We conclude that for Si dangling-bond defects hyperfine interactions calculated with the Hartree-Fock scheme are generally larger than those obtained with a GGA-DFT scheme and that the size of the differences depends on the specific system under consideration. This conclusion is consistent with observations in a previous investigation of E'-type centers,[39,70] in which a stronger spin-localization

TABLE IV. Hyperfine values (in Gauss) for small cluster models as calculated with three different electronic-structure methods: one pseudopotential (PP) and two all-electron methods (DMOL and GAUSSIAN 98). The detailed description of the size and the composition of the clusters is given in the text.

		PP	DMOL		GAUSSIAN 98	
			Full	Frozen core	Full	Valence only
$\cdot Si{\equiv}Si_3$	a_{HF}	118	98	104	78	87
	a^N_{HF}	−3	−5	−5	−4	−4
$\cdot Si{\equiv}Si_2O$	a_{HF}	162	148	152	129	135
	a^N_{HF}	16	16	16	14	15
$\cdot Si{\equiv}SiO_2$	a_{HF}	242	218	223	207	211
	a^N_{HF}	77	64	65	65	66
$\cdot Si{\equiv}O_3$	a_{HF}	424	407	413	389	391

tendency of the Hartree-Fock scheme was observed. Indeed, this tendency explains the behavior of the differences as a function of the number of first-neighbor oxygen atoms. The increase of the hyperfine interaction due to oxygen neighbors dominates the Hartree-Fock spin-localization effect, and the latter plays a smaller role as the number of oxygen atoms increases.

B. Role of core polarization

Although we could properly reconstruct the valence charge density,[30,57] effects associated to the polarization of the core wave functions could not be accounted for in our PP method. We here provide an estimate of such core-polarization effects by using AE methods and comparing with the PP method.

All the calculations in this section were carried out within the PW91 GGA-DFT scheme or an equivalent (see Sec. II). We adopted the same kind of clusters as in the previous section and used three different electronic-structure methods: the same PP method as used for the periodic model structures and two AE methods (G98 and DMOL). For each electronic-structure method, the same kinds of clusters as in the previous section were relaxed and their hyperfine parameters calculated.[69] Our results are summarized in Table IV. All the methods show hyperfine interactions a_{HF} increasing with the number of first-neighbor oxygen atoms. However, significantly different values for a_{HF} are obtained with different methods, particularly for the cluster with the $\cdot Si{\equiv}Si_3$ unit. The SHF interaction a^N_{HF} is found to depend less on the applied method.

The DMOL code offers the possibility of calculating hyperfine parameters in two ways, either in a full AE mode or in a frozen-core approximation. The comparison between these two calculation modes directly provides an estimate of core-polarization effects, which is not subject to uncertainties associated to the use of different methodological frameworks. As can be seen in Table IV, the frozen-core calculations always overestimate the full AE results, indicating that core-polarization effects give a negative contribution to the isotropic hyperfine interactions. The size of this effect is as large as 6% for three Si neighbors and decreases monotonically until 1% with an increasing number of first-neighbor oxygen atoms. In particular, core polarization affects the hyperfine interactions, both a_{HF} and a^N_{HF}, for the cluster with a $\cdot Si{\equiv}SiO_2$ core unit by only $\sim 2\%$.

TABLE V. Isotropic hyperfine interactions (in Gauss) calculated for small cluster models differing by the termination at the oxygen atoms, compared to the results for the periodic structure models.

		Cluster termination		Periodic
		−H	$-SiH_3$	model
$\cdot Si{\equiv}Si_2O$	a_{HF}	153	162	
	a^N_{HF}	17	16	
$\cdot Si{\equiv}SiO_2$	a_{HF}	210	242	315
	a^N_{HF}	78	77	202
$\cdot Si{\equiv}O_3$	a_{HF}	340	424	499

The results obtained with the PP and the frozen-core DMOL methods compare well, showing differences of at most 12%. However, the DMOL frozen-core approximation appears to systematically underestimate the results obtained with the PP method, the largest difference of 12% being found for the cluster with the $\cdot Si{\equiv}Si_3$ core unit. In this respect, it is useful to mention that, in a previous investigation based on DMOL, hyperfine parameters for two systems containing this unit, i.e., the P_b defect and the $\cdot SiH_3$ cluster, were found to underestimate experimental values by about 10%.[71]

The results obtained with the G98 code give hyperfine parameters which are substantially smaller than both those obtained with the DMOL code and with the PP method. This effect could conceivably result from the inherent inability of Gaussian-type basis functions to describe cusps of the wave functions at the nucleus site.[57] We were not able to perform frozen-core calculations with the G98 code, but we could derive the contribution to the isotropic hyperfine interaction from core and valence orbitals separately (Table IV). The core-polarization effect estimated in this way varies from 11% for the $\cdot Si{\equiv}Si_3$ unit to 1% for the $\cdot Si{\equiv}O_3$, consistent with the DMOL results.

In summary, we found that core polarization affects hyperfine interactions of silicon dangling-bond defects in a quantitatively different way according to the number of oxygen neighbors. The effect is largest for the $\cdot Si{\equiv}Si_3$ unit (6% to 11%) and becomes negligible for the $\cdot Si{\equiv}O_3$ unit (1%). Furthermore, our study shows that hyperfine parameters obtained with various electronic-structure methods differ considerably, pointing out that it is more difficult to obtain converged values for such parameters than for energies and structural parameters. In particular, the G98 code gave results which were significantly smaller than those obtained with DMOL and the PP method.

C. Caveats when adopting small cluster models

1. Size effects

Previous theoretical work on Si dangling-bond defects was carried out with cluster models of minimal size: $\cdot Si(SiH_3)_{3-x}(OH)_x$ (with $0 \leqslant x \leqslant 3$).[40,42] In order to estimate size effects, we calculated hyperfine interactions, for two sets of clusters differing by the termination of the oxygen atoms: $-H$ and $-SiH_3$. In this section, we used the PP method.

Our results are collected in Table V. Very significant differences are found between the hyperfine interactions for the two sets of clusters. The clusters with $-SiH_3$ terminations yielded hyperfine values a_{HF} larger by 6%, 15%, and 25% than those for the clusters with $-H$ terminations when going from one to three first-neighbor oxygen atoms. This effect can be explained by the larger electron affinity of the $-OSiH_3$ group with respect to the $-OH$ group. On the contrary, SHF interactions a_{HF}^{N} were found to be relatively insensitive to the cluster termination at the oxygen atoms. In fact, for Si^{N} atoms, changes to such terminations only modify their third-neighbor shell.

2. Strain effects

The Si-Si bond lengths and the bond angles around the defect Si atoms reflect a more strained defect center in the periodic as compared to the cluster model structures. This is an expected consequence of the interaction between the defect core unit and the SiO_2 network, which is generally underestimated in cluster calculations. Here we would like to point out that the correct modeling of strain effects is critical for the SHF interaction a_{HF}^{N} of the $\cdot Si \equiv SiO_2$ defect center. Note that the value for this interaction is smaller for the cluster than for the periodic models by almost a factor of 3.

Strain effects might also occur in periodic structure models either because of the limited size of the unit cell or because of the defect generation procedure. For this reason, we could not model the $\cdot Si \equiv OSi_2$ center using the periodic model structure of amorphous SiO_2 available to us.

3. Polarization effects

When comparing hyperfine interactions calculated for the clusters with those for the periodic models, we observed that the latter yield significantly larger values (Table V). These differences appeared too large to be assigned solely to cluster size and local strain effects. In fact, we determined that yet another cause associated to the dangling-bond environment could contribute to increasing the hyperfine interaction. Indeed, our calculations show that the dangling bond could noticeably be perturbed by oxygen atoms belonging to its surrounding cage structure. The interaction is mainly a Pauli repulsion, which decreases the *p* character of the dangling-bond orbital, thereby increasing the Fermi contact interaction. Because of the amorphous nature of the system, it is difficult to provide a statistically accurate value for this effect. Test calculations showed that a single oxygen atom at a distance of 3.5 Å from the defect center causes an enhancement of the contact interaction of about 15%.

The present study shows that the quantitative estimates obtained with small cluster models should not be relied upon when assigning defects such as the *S* and *X* centers. In particular, small-sized cluster models do not incorporate most of the important structural aspects of the defect environment. However, cluster calculations might be useful for qualitative predictions and to reveal trends. In fact, we found that the cluster calculations qualitatively reproduced all the trends obtained for the periodic cluster models. In particular, the extensive delocalization of the spin density in the case of the $\cdot Si \equiv SiO_2$ defect center is well reproduced by the cluster calculations.

VI. CONCLUSIONS

We investigated Si dangling-bond defects in amorphous SiO_2, using a pseudopotential method based on density-functional theory and periodic model structures. In particular, we focused on defect centers featuring $\cdot Si \equiv O_3$ and $\cdot Si \equiv SiO_2$ core units. Comparison with ESR experiments was made possible through the generation of fully relaxed atomic structure models and the calculation of hyperfine parameters.

The defect center with a $\cdot Si \equiv O_3$ core unit corresponds to the generally accepted model for the E'_γ center. We found overall good agreement with experiment for both hyperfine and superhyperfine interactions. The overestimation by about 20% of the principal hyperfine interaction corresponds to the accuracy of our approach. Since core polarization for the $\cdot Si \equiv O_3$ unit is of the order of 1% (Sec. V), we conclude that most of this error results from the neglect of relativistic effects[58] or to a deficiency of our density-functional scheme.[50] We also showed that the $\cdot Si \equiv O_3$ defect centers exhibit identical hyperfine interactions in the neutral and positively charged states, in accord with experimental observations.[3,9,10,15,16]

As far as the $\cdot Si \equiv SiO_2$ defect center is concerned, our calculations indicate that the associated ESR spectrum should contain two doublets of equal intensity, with calculated splittings of 202 and 315 G. Because of the strong sensitivity of the smaller hyperfine interaction to the bond length of the Si-Si backbond, the associated hyperfine line in the ESR spectrum is expected to be broader. The cluster calculations indicate that also for this defect core-polarization effects should be small (2%). In view of the differences between theoretical and experimental hyperfine parameters observed for the E'_γ center and assuming a systematic behavior of the error, we expect that our calculated values overestimate experimental values by about 20%. Furthermore, we expect a larger error for the secondary hyperfine interaction, in view of its strong sensitivity to the $Si\text{-}Si^{N}$ bond length and the limited statistics in our study.

The features associated to the $\cdot Si \equiv SiO_2$ unit appear to be all reunited in the experimental characterization of the *S* center.[24] Although at the limit of experimental accuracy, the hyperfine spectrum of this defect center shows two hyperfine doublets at 162 and 279 G, the inner with an apparent weaker intensity barely distinguishable from the background. Another candidate defect, known as the *X* center,[26] shows a

single hyperfine doublet at 230 G, and appears less suited to be assigned to a $\cdot Si{\equiv}SiO_2$ both for the quantitative value of its main hyperfine interaction and for the absence of a secondary doublet in the ESR spectrum.

The presence of two oxygen atoms in the first-neighbor shell of the defect atom is at the origin of the spin-delocalization effect in the $\cdot Si{\equiv}SiO_2$ unit. Their strong electronegativity enhances the mixing between the dangling-bond orbital and the bonding orbital in the Si-Si backbond. Preliminary cluster calculations (not described here) indicate that such a spin-delocalization phenomenon is not only characteristic of SiO_2 systems, but also occurs for Si dangling-bond kernels containing other highly electronegative atoms in the first-neighbor shell, such as N or F.

In the present work, we did not attempt to model the $\cdot Si{\equiv}Si_2O$ using periodic models, because the generated strain could poorly be accommodated in the model structure of amorphous SiO_2 available to us. Extrapolating from our results for small cluster models (Table V), we could obtain estimates for the hyperfine interaction associated to the $\cdot Si{\equiv}Si_2O$ unit. Since such estimates fall close to the hyperfine splitting of the inner doublet of the *S* center,[24] we cannot fully rule out such an assignment.

Our investigation is complemented by an extended study of cluster models in which hyperfine interactions as obtained with various electronic-structure methods are compared. Several conclusions could be drawn from this cluster investigation. First, we assessed the importance of the core-polarization contribution to the hyperfine interactions associated to Si dangling-bond defects in SiO_2. We found that core polarization is most important for the $\cdot Si{\equiv}Si_3$ center (6% to 11%) and that its effect decreases for increasing numbers of oxygen atoms in the first-neighbor shell. In this way, we could provide an estimate of this effect, which is neglected in our pseudopotential method. Second, the cluster study allowed us to compare our results with previous theoretical work on Si dangling-bond defects in amorphous SiO_2.[40,42] In this respect, we analyzed separately the effects resulting from the use of the Hartree-Fock approximation, the G98 code, and the choice of minimal size clusters, and showed that each of these effects might be the cause of unreliable quantitative estimates. We arrived at the conclusion that small cluster calculations well describe trends but should not be relied upon for a quantitative comparison with experimental data. Third, the comparison between the calculated hyperfine interactions for the small cluster and the periodic structure models allowed us to recognize the role of the amorphous environment. In addition to the usual size effects, we found that hyperfine interactions are significantly affected by strain and cage-polarization effects.

ACKNOWLEDGMENTS

Financial support from the Bolyai Fellowship, the OTKA Grant No. T34547 (A.S.), and from the Swiss National Science Foundation under Grant No. 620-57850.99 (A.P.) are greatly acknowledged. The calculations were performed on the NEC-SX4 of the Swiss Center for Scientific Computing (CSCS) in Manno.

*Present address: Centro Svizzero di Calcolo Scientifico (CSCS), Via Cantonale, CH-6928 Manno, Switzerland.

[1] E.H. Poindexter and W.L. Warren, J. Electrochem. Soc. **142**, 2508 (1995).
[2] R.A. Weeks, J. Non-Cryst. Solids **179**, 1 (1994).
[3] J.F. Conley, Jr., P.M. Lenahan, H.L. Ewans, R.K. Lowry, and T.J. Morthorst, J. Appl. Phys. **76**, 2872 (1994).
[4] F.J. Feigl, W.B. Fowler, and K.L. Yip, Solid State Commun. **14**, 225 (1974).
[5] J.K. Rudra and W.B. Fowler, Phys. Rev. B **35**, 8223 (1987).
[6] D.L. Griscom, Phys. Rev. B **20**, 1823 (1979).
[7] D.L. Griscom, Phys. Rev. B **22**, 4192 (1980).
[8] V.V. Afanas'ev and A. Stesmans, J. Phys.: Condens. Matter **12**, 2285 (2000).
[9] W.L. Warren, P.M. Lenahan, B. Robinson, and J.H. Stathis, Appl. Phys. Lett. **53**, 482 (1988).
[10] V.V. Afanas'ev, J.M.M. de Nijs, P. Balk, and A. Stesmans, J. Appl. Phys. **78**, 6481 (1995).
[11] M.E. Zvanut, F.J. Feigl, W.B. Fowler, J.K. Rudra, P.J. Caplan, E.H. Poindexter, and J.D. Zook, Appl. Phys. Lett. **54**, 2118 (1989).
[12] D. Herve, J.-L. Leray, and R.A.B. Devine, J. Appl. Phys. **72**, 3634 (1992).
[13] B.J. Mrstik, V.V. Afanas'ev, A. Stesmans, P.J. McMarr, and R.K. Lawrence, J. Appl. Phys. **85**, 6577 (1999).
[14] V.V. Afanas'ev, A. Stesmans, A.G. Revesz, and H.L. Hughes, J. Electrochem. Soc. **145**, 3157 (1998).
[15] D.L. Griscom, Nucl. Instrum. Methods Phys. Res. B **1**, 481 (1984).
[16] D.L. Griscom, J. Non-Cryst. Solids **73**, 51 (1985).
[17] T. Uchino, M. Takahashi, and T. Yoko, Phys. Rev. B **62**, 2983 (2000).
[18] T. Uchino, M. Takahashi, and T. Yoko, Phys. Rev. Lett. **86**, 5522 (2001).
[19] E. Holzenkämpfer, P.W. Richter, J. Stuke, and U. Voget-Grote, J. Non-Cryst. Solids **32**, 327 (1979).
[20] D.L. Griscom, E.J. Friebele, J.K. Long, and J.W. Fleming, J. Appl. Phys. **54**, 3743 (1983).
[21] A. Stesmans, B. Nouwen, and V.V. Afanas'ev, Phys. Rev. B **58**, 15 801 (1998).
[22] A. Stesmans and V.V. Afanas'ev, Appl. Phys. Lett. **69**, 2056 (1996).
[23] A. Stesmans and V.V. Afanas'ev, Microelectron. Eng. **36**, 201 (1997).
[24] A. Stesmans, B. Nouwen, and V.V. Afanas'ev, Appl. Phys. Lett. **80**, 4753 (2002); Phys. Rev. B **66**, 045307 (2002).
[25] H. Hosono and R.A. Weeks, Phys. Rev. B **40**, 10 543 (1989).
[26] H. Hosono, H. Kawazoe, K. Oyoshi, and S. Tanaka, J. Non-Cryst. Solids **179**, 39 (1994).
[27] D.L. Griscom, E.J. Friebele, and G.H. Sigel, Jr., Solid State Commun. **15**, 479 (1974).
[28] E.H. Poindexter and P.J. Caplan, Prog. Surf. Sci. **14**, 201 (1983).
[29] A.H. Edwards and W.B. Fowler, Microelectron. Reliab. **39**, 3 (1999).

[30] A. Stirling, A. Pasquarello, J.-C. Charlier, and R. Car, Phys. Rev. Lett. **85**, 2773 (2000); *Physics and Chemistry of* SiO_2 *and the* Si-SiO_2 *Interface-4*, edited by H. Z. Massoud, I. J. R. Baumvol, M. Hirose, and E. H. Poindexter (Electrochemical Society, New York, 2000), p. 283.
[31] E.P. O'Reilly and J. Robertson, Phys. Rev. B **27**, 3780 (1983).
[32] A.H. Edwards, W.B. Fowler, and F.J. Feigl, Phys. Rev. B **37**, 9000 (1988).
[33] K.C. Snyder and W.B. Fowler, Phys. Rev. B **48**, 13 238 (1993).
[34] D.C. Allan and M.P. Teter, J. Am. Ceram. Soc. **73**, 3247 (1990).
[35] M. Boero, A. Pasquarello, J. Sarnthein, and R. Car, Phys. Rev. Lett. **78**, 887 (1997).
[36] G. Pacchioni and G. Ieranò, Phys. Rev. B **56**, 7304 (1997).
[37] G. Pacchioni, G. Ieranò, and A.M. Márquez, Phys. Rev. Lett. **81**, 377 (1998).
[38] A. Courtot-Descharles, P. Paillet, and J.L. Leray, J. Non-Cryst. Solids **245**, 154 (1999).
[39] G. Pacchioni and M. Vitiello, J. Non-Cryst. Solids **245**, 175 (1999).
[40] S.P. Karna and H.A. Kurtz, Microelectron. Eng. **48**, 109 (1999).
[41] A.C. Pineda and S.P. Karna, J. Phys. Chem. A **104**, 4699 (2000).
[42] S. P. Karna, H. A. Kurtz, A. C. Pineda, W. M. Shedd, and R. D. Pugh, in *Defects in* SiO_2 *and Related Dielectrics: Science and Technology*, edited by G. Pacchioni, D. L. Griscom, and L. Skuja (Kluwer Academic, New York, 2000).
[43] C.M. Carbonaro, V. Fiorentini, and F. Bernardini, Phys. Rev. Lett. **86**, 3064 (2001).
[44] D. Donadio, M. Bernasconi, and M. Boero, Phys. Rev. Lett. **87**, 195504 (2001).
[45] P.E. Blöchl, Phys. Rev. B **62**, 6158 (2000).
[46] C.J. Pickard and F. Mauri, Phys. Rev. Lett. **88**, 086403 (2002).
[47] T. Uchino, Curr. Opin. Solid State Mater. Sci. **5**, 517 (2001).
[48] J. Sarnthein, A. Pasquarello, and R. Car, Phys. Rev. Lett. **74**, 4682 (1995); Phys. Rev. B **52**, 12 690 (1995).
[49] W. Kohn and L.J. Sham, Phys. Rev. **140**, A1133 (1965).
[50] J.P. Perdew, J.A. Chevary, S.H. Vosko, K.A. Jackson, M.R. Pederson, D.J. Singh, and C. Fiolhais, Phys. Rev. B **46**, 6671 (1992).
[51] R. Car and M. Parrinello, Phys. Rev. Lett. **55**, 2471 (1985).
[52] D. Vanderbilt, Phys. Rev. B **41**, 7892 (1990).
[53] A. Pasquarello, K. Laasonen, R. Car, C. Lee, and D. Vanderbilt, Phys. Rev. Lett. **69**, 1982 (1992); K. Laasonen, A. Pasquarello, R. Car, C. Lee, and D. Vanderbilt, Phys. Rev. B **47**, 10 142 (1993).
[54] A. Pasquarello and R. Car, Phys. Rev. Lett. **80**, 5145 (1998).
[55] J. Sarnthein, A. Pasquarello, and R. Car, Science **275**, 1925 (1997); A. Pasquarello and R. Car, Phys. Rev. Lett. **79**, 1766 (1997); A. Pasquarello, J. Sarnthein, and R. Car, Phys. Rev. B **57**, 14 133 (1998); A. Pasquarello, *ibid.* **61**, 3951 (2000); P. Umari and A. Pasquarello, Physica B **316-317**, 572 (2002).
[56] C.G. Van de Walle and P.E. Blöchl, Phys. Rev. B **47**, 4244 (1993).
[57] B. Hetényi, F. De Angelis, P. Giannozzi, and R. Car, J. Chem. Phys. **115**, 5791 (2001).
[58] S. Blügel, H. Akai, R. Zeller, and P.H. Dederichs, Phys. Rev. B **35**, 3271 (1995).
[59] Computer code DMOL, 3.0.0 version, (Biosym/MSI, San Diego, CA, 1995).
[60] M. J. Frisch, G. W. Trucks, H. B. Schlegel, G. E. Scuseria, M. A. Robb, J. R. Cheeseman, V. G. Zakrzewski, J. A. Montgomery, Jr., R. E. Stratmann, J. C. Burant, S. Dapprich, J. M. Millam, A. D. Daniels, K. N. Kudin, M. C. Strain, O. Farkas, J. Tomasi, V. Barone, M. Cossi, R. Cammi, B. Mennucci, C. Pomelli, C. Adamo, S. Clifford, J. Ochterski, G. A. Petersson, P. Y. Ayala, Q. Cui, K. Morokuma, D. K. Malick, A. D. Rabuck, K. Raghavachari, J. B. Foresman, J. Cioslowski, J. V. Ortiz, B. B. Stefanov, G. Liu, A. Liashenko, P. Piskorz, I. Komaromi, R. Gomperts, R. L. Martin, D. J. Fox, T. Keith, M. A. Al-Laham, C. Y. Peng, A. Nanayakkara, C. Gonzalez, M. Challacombe, P. M. W. Gill, B. Johnson, W. Chen, M. W. Wong, J. L. Andres, C. Gonzalez, M. Head-Gordon, E. S. Replogle, and J. A. Pople, Computer code GAUSSIAN 98, Revision A.6 (Gaussian, Inc., Pittsburgh PA, 1998).
[61] A.D. Becke, Phys. Rev. A **38**, 3098 (1988).
[62] B. Delley, J. Chem. Phys. **92**, 508 (1990).
[63] A.V. Shendrik and D.M. Yudin, Phys. Status Solidi B **85**, 43 (1978).
[64] M.G. Jani, R.B. Bossoli, and L.E. Halliburton, Phys. Rev. B **27**, 2285 (1983).
[65] A. Kalnitsky, J.P. Paul, E.H. Poindexter, P.J. Caplan, R.A. Lux, and E.R. Boothroyd, J. Appl. Phys. **67**, 7359 (1990).
[66] A. Pasquarello, Appl. Surf. Sci. **166**, 451 (2000).
[67] H.A. Bent, Chem. Rev. **61**, 275 (1961).
[68] See, for instance, T. W. G. Solomons, *Organic Chemistry*, 6th ed. (Wiley, New York, 1996).
[69] Structural differences between clusters relaxed with different schemes or methods are minor and do not affect hyperfine parameters significantly.
[70] G. Pacchioni and C. Mazzeo, Phys. Rev. B **62**, 5452 (2000).
[71] B. Tuttle, Phys. Rev. B **60**, 2631 (1999). In particular, we here reproduced the DMOL results for the $\cdot SiH_3$ cluster given in the later paper.
[72] M. Cook and C.T. White, Phys. Rev. B **38**, 9674 (1988).